Regular Article

PHYSICAL CHEMISTRY RESEARCH
Published by the
Iranian Chemical Society
www.physchemres.org
info@physchemres.org

Phys. Chem. Res., Vol. 9, No. 3, 373-384, September 2021
DOI: 10.22036/pcr.2021.257894.1856

Comparative Study of Glyphosate Adsorption on Armchair CNT(5.5) and BNNT(5.5): A DFT Study

S. Bouhara[a,b,*] and D. Hammoutène[b]

[a]*National School of Built and Ground Works Engineering, B.P. 32, Kouba, Algiers, Algeria*
[b]*USTHB, Laboratory of Thermodynamics and Molecular Modeling, Faculty of Chemistry, B.P. 32 El Alia, 16111 Bab Ezzouar, Algiers, Algeria*

(Received 18 November 2020, Accepted 26 March 2021)

Detecting glyphosate is of great importance as it has been classified as a probable carcinogen. In literature, many nanotubes, including carbon nanotube (CNT), have been used to detect glyphosate (Glyp). However, no study has been conducted on boron nitride nanotube (BNNT) as an adsorbate for Glyp. So, this work focuses on performing a comparative study on the Glyp adsorption on CNT(5.5) and BNNT(5.5) using B3LYP, M06-2X and ωB97X-D/6-31G(d) by first-principle calculations in the framework of Density Functional Theory. Based on the results, the adsorption energies of BNNT(5.5)/Glyp are slightly higher than those of CNT(5.5)/Glyp and are in very close agreement with the NCI analysis. The thermodynamic parameters also showed that the two nanotubes could detect glyphosate with a physisorption process that was exothermic and thermodynamically favourable. In addition, TDOS and QTAIM analyses revealed the non-covalent interaction between glyphosate and the two nanotubes.

Keywords: Glyphosate, Boron nitride nanotube, Carbon nanotube, DFT, QTAIM and TDOS

INTRODUCTION

Glyphosate (Glyp), [N-(phosphonomethyl) glycine], is a non-selective herbicide and one of the most widely used substances in agriculture worldwide. It can inhibit some enzymes in unwanted plants [1]. The extended half-life of Glyp [2] and its long persistence in soil and water [2-5] may increase the risk of long-term environmental contamination and its affect on the human health. In March 2015, the International Agency for Research on Cancer classified glyphosate as a probable carcinogen [6]. Besides, the review by Mesnage *et al.* reports that glyphosate has tumorigenic, teratogenic, and neurological and hepatorenal effects [7]. Recently, Pu *et al.* found that exposure of pregnant women to glyphosate can induce autistic behaviour in the offspring [8].

Lately, detecting glyphosate has become very important using several techniques such as HPLC [9], fluorescence [10], spectrophotometry [11], photocatalysis [12,13] and electrochemistry [14,15].

Nanotubes are typically appropriate for sensor applications due to their large surface-to-volume ratio and porous surface [16-19]. Consequently, they are used to detect and degrade glyphosate due to their high sensibility and specificity for this herbicide. Carbon nanotubes (CNTs) exhibit high performance due to their excellent chemical, physical and mechanical properties [20,21]. Therefore, many studies have used CNTs for the detection of glyphosate. A copper phthalocyanine/multi-walled carbon nanotube (MWCNT) film electrode is used to determine the glyphosate's concentration in a range from 0.83-9.90 µM with a detection limit of 12.2 nM [20]. Likewise, Oliveira *et al.* have developed a biosensor based on peroxidase immobilized on nanoclay, which is associated with carbon nanotubes for the determination of glyphosate [21]. In addition, CuO/MWCNTs are expanded to detect glyphosate

*Corresponding author. E-mail: bouharasafia@yahoo.fr

by fluorescence [22]. Also, the Al/MWCNT/O_2 system is used to generate H_2O_2 which could lead to the degradation of glyphosate [23]. Furthermore, Zhang *et al.* used MWCNTs combined with UHPLC to detect glyphosate and glufosinate in corn simultaneously [24]. Although carbon nanotubes are widely used, their electrical properties (metallic or semiconductor) depend on tube diameter and chirality [25-27]. Boron nitride nanotubes (BNNTs) have become alternative candidates for CNTs, because their electrical properties (inorganic semiconductor) are independent of chirality and diameter, unlike CNTs electrical properties.

In addition, they exhibit high resistance to oxidation, hardness, high mechanical strength, high thermal stability, and conductivity with heat resistance compared to CNTs [26,28,29]. This makes them one of the most favourable materials for nanotechnology applications [30].

Therefore, this study focuses on the BNNT interactions with glyphosate. To the best of our knowledge, there are no theoretical and experimental data in the literature related to the glyphosate adsorption on BNNTs. So, we tried to find answers to the following questions: can BNNT adsorb Glyp more than CNT? and, what is the nature of interaction between BNNT and glyphosate?

COMPUTATIONAL METHODS

The structures of the CNT(5.5) and BNNT(5.5) were designed by tubegen [31] software. The terminal atoms of the nanotubes were saturated with hydrogen atoms to avoid border effects. The formulas of CNT(5.5) and BNNT(5.5) are respectively $C_{60}H_{20}$ and $B_{30}H_{20}N_{30}$. All the density functional theory (DFT) calculations in this paper were performed using the Gaussian 16 package [32]. The full geometry optimization of CNT(5.5) and BNNT(5.5) in the absence and presence of glyphosate was performed using three different DFT functionals: B3LYP, M06-2X and ωB97X-D accompanied by a 6-31G(d) basis set. B3LYP has been commonly used for nanostructures [29,33,34]. M06-2X is a global hybrid meta-GGA functional with 54% of Hartree-Fock (HF) exchange, it gives good results for non-covalent interactions [35]. ωB97X-D is a long-range corrected hybrid with dispersion corrections and 100% of HF exchange. It leads to a satisfactory accuracy for thermochemistry and non-covalent interactions [36].

The optimized geometries' frequency calculations confirmed that all structures were stationary points, with no imaginary frequencies (the values of frequencies are given on supplementary data).

The adsorption energies (E_{ads}) of Glyp at the surface of the nanotubes were calculated as follows:

$$E_{ads} = E_{tube/Glyp} - (E_{tube} + E_{Glyp}) \quad (1)$$

where $E_{tube/Glyp}$, E_{tube} and E_{Glyp} are the total energies of the nanotube/Glyp complex, nanotube, and glyphosate, respectively.

To better understand the intermolecular interaction between nanotubes and glyphosate, analyses of total density of states (TDOS), quantum theory of atoms in molecules (QTAIM) [37], and non-covalent interaction (NCI) [38] were performed by the Multiwfn program [39] at the ωB97X-D/6-31g(d) level of theory.

RESULTS AND DISCUSSIONS

Optimization of CNT(5.5)/glyphosate and BNNT(5.5)/glyphosate complexes was carried out at the B3LYP/6-31g(d), M06-2X/6-31g(d), and ωB97X-D/6-31g(d) level. To explore the effect of nanotube diameter and length on the amount of adsorption energy, we increased the diameter of BNNT to armchair (7.7) and increased the length of BNNT(5.5) to ($B_{60}H_{20}N_{60}$). The adsorption energy of Glyp from BNNT(5.5) to BNNT(7.7) increases by 5.93%, which is not significant. Also, the increase in length implies an increase in E_{ads} by little amount of ≈16 kJ mol^{-1}. Therefore, the selection of the $B_{30}H_{20}N_{30}$ armchair (5.5) nanotube is suitable and rational in terms of computational cost (see supplementary data). The ωB97X-D/6-31G(d)-optimized geometries of complexes are illustrated in Fig. 1.

The adsorption energy is calculated for all the optimized structures using B3LYP/6-31g(d), M06-2X/6-31g(d) and ωB97X-D/6-31g(d). All calculated adsorption energies are summarised in Table 1.

We observed that the adsorption energies of BNNT(5.5)/glyphosate are slightly more negative than those calculated for CNT(5.5)/glyphosate. Moreover, the ωB97X-D functional gives the most negative value of the adsorption

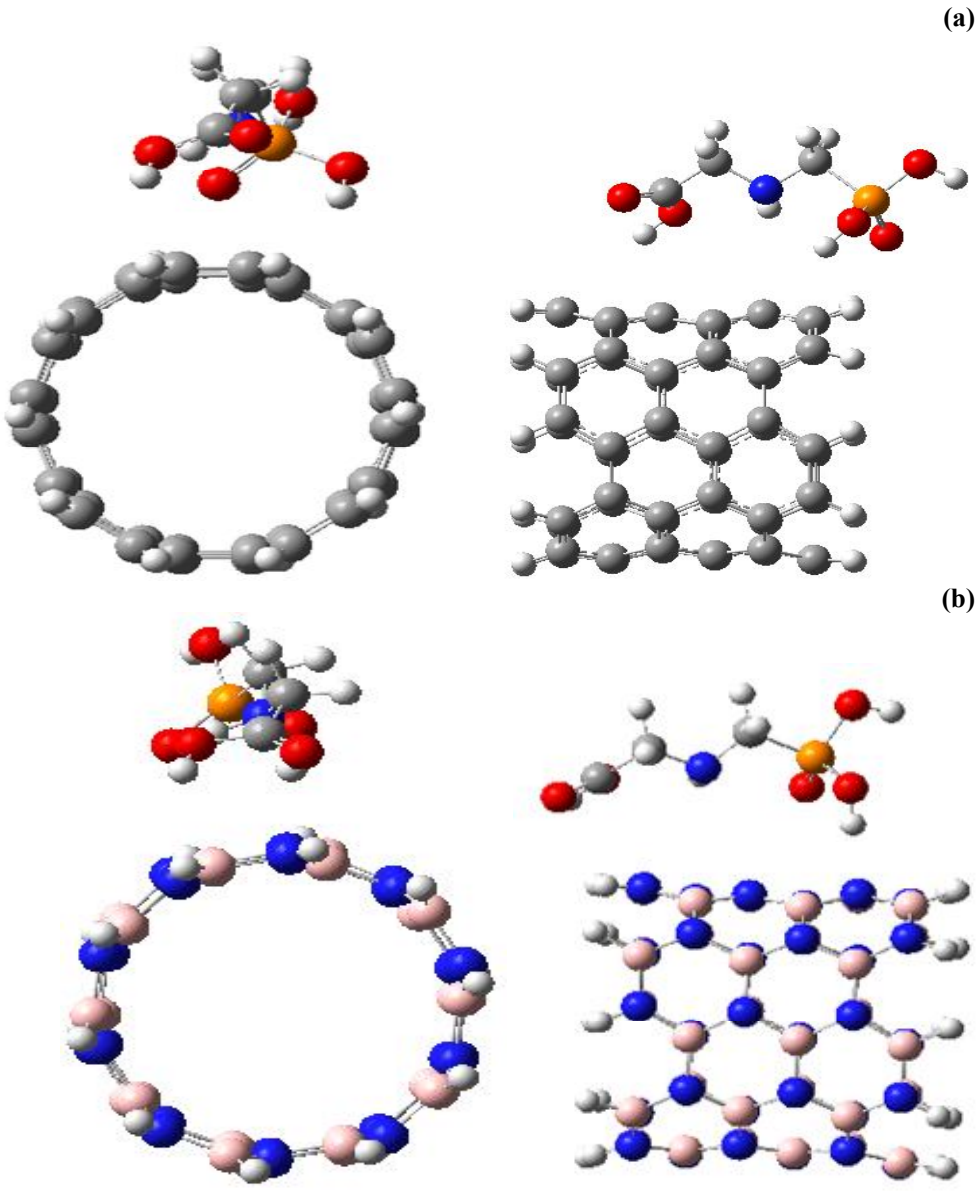

Fig. 1. The relaxed structures obtained from glyphosate adsorption onto the surfaces of (a) CNT(5.5) and (b) BNNT(5.5) at the ωB97X-D/6-31g(d) level of theory.

energy. Therefore, we can conclude that the non-covalent interactions were better taken into account by ωB97X-D compared to B3LYP and M06-2X. Therefore, we chose ωB97X-D for the basis set superposition errors (BSSE), thermochemistry calculations, DOS, QTAIM and NCI analyses. The basis set superposition errors have been estimated for the counterpoise correction [40].

In Table 2, the calculated parameters such as BSSE, HOMO, LUMO, energy gap and chemical potential (μ) before and after glyphosate adsorption on CNT(5.5) and

Table 1. Adsorption Energies (kJ mol^{-1}) for CNT(5.5)/Glyphosate and BNNT(5.5)/Glyphosate Complexes

E_{ads} (kJ mol^{-1})	Adsorption energy (E_{ads}) (kJ mol^{-1})		
	B3LYP/6-31G(d)	M06-2X/6-31G(d)	ωB97X-D/6-31G(d)
CNT(5.5)/Glyphosate	-28.79	-56.91	-62.09
BNNT(5.5)/Glyphosate	-31.68	-57.99	-67.21

Table 2. BSSE (in kJ mol^{-1}), HOMO, LUMO, Energy Gap (E_g) and Chemical Potential (μ) (in eV) before and after Glyphosate Adsorption on CNT(5.5) and BNNT(5.5) Calculated by ωB97X-D/6-31G(d)

Optimized systems	BSSE (kJ mol^{-1})	HOMO (eV)	LUMO (eV)	E_g (eV)	μ (eV)
CNT(5.5)		-7.92	-6.99	0.93	-7.45
CNT(5.5)/Glyp	21.28	-7.93	-6.99	0.94	-7.46
BNNT(5.5)		-9.95	-4.04	5.91	-6.99
BNNT(5.5)/Glyp	27.03	-9.16	-4.05	5.11	-6.60

BNNT(5.5) are collected.

The energy gap (E_g) and chemical potential (μ) were calculated using the following equations:

$$Eg = HOMO - LUMO \quad (2)$$

$$\mu = \frac{(HOMO + LUMO)}{2} \quad (3)$$

Table 2 shows that the energy gap value calculated for CNT(5.5) before and after adsorption is almost the same, which indicates that CNT(5.5) is not sensitive to glyphosate, whereas, in the case of BNNT(5.5), we observed a decrease of 0.8 in the E_g after glyphosate adsorption. This decrease in E_g increased electrical conductivity and made BNNT(5.5) more sensitive to detect glyphosate than CNT(5.5).

To confirm these conclusions and further study the effects of glyphosate adsorption on the electronic properties of CNT and BNNT, TDOS plots were also analyzed for the complexes and compared to the DOS isolated nanotubes (Fig. 2). The TDOS spectra revealed that, after adsorption, the conduction levels are shifted to a slightly higher energy level; therefore, this change in conductance involves an electrical signal which can be used for sensing glyphosate.

Furthermore, no variation was noted within the energy gap, indicating the weak interaction between Glyp and the nanotubes. It is also noted that the conduction level of BNNT(5.5)/glyphosate is slightly higher than that of CNT(5.5)/glyphosate, which is in concordance of results found in Table 2.

To assess the thermodynamic feasibility of the glyphosate adsorption on nanotubes, we calculated some thermochemical parameters, including enthalpy (ΔH), free energy (ΔG), and entropy (ΔS), according to the following

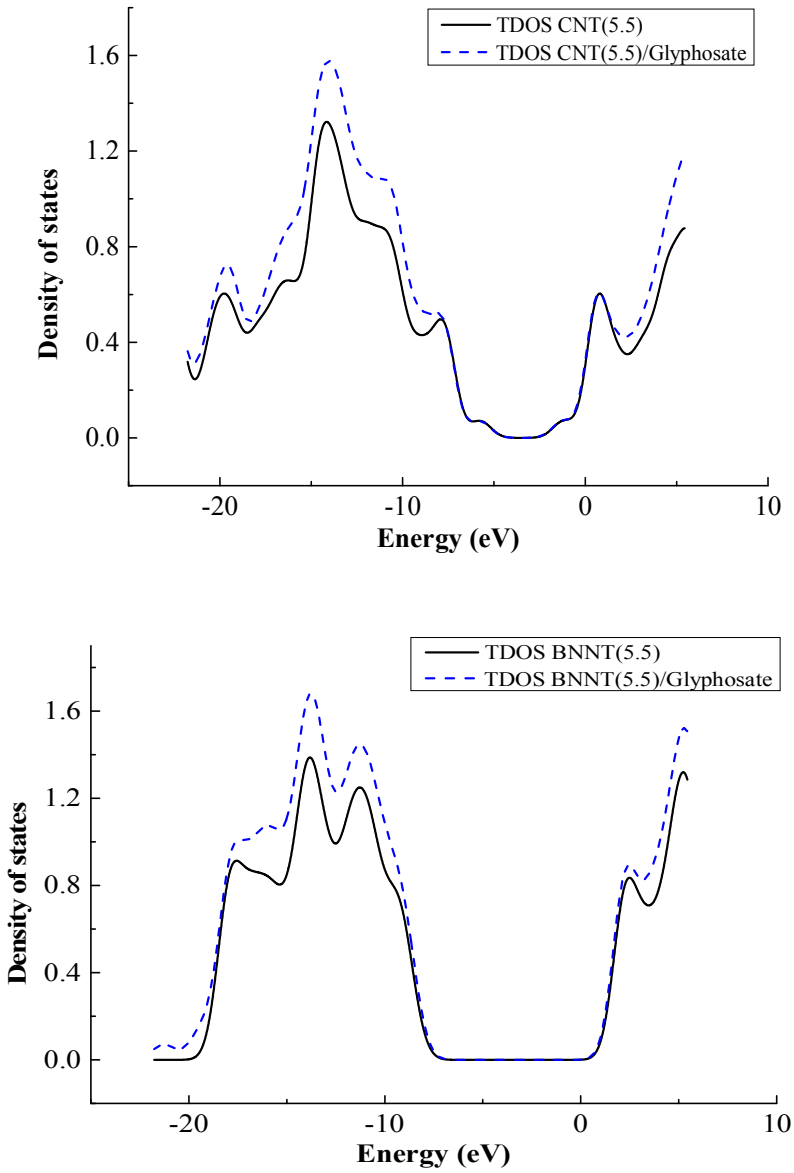

Fig. 2. The total electronic density of states (TDOS) for CNT(5.5), BNNT(5.5) and tubes/glyphosate complexes obtained at the ωB97X-D/6-31G(d) level.

relationships:

$$\Delta H_{ads} = H_{tube/Glyp} - H_{tube} - H_{Glyp} \quad (4)$$

$$\Delta G_{ads} = G_{tube/Glyp} - G_{tube} - G_{Glyp} \quad (5)$$

$$\Delta S_{ads} = S_{tube/Glyp} - S_{tube} - S_{Glyp} \quad (6)$$

where H, G and S are respectively thermal enthalpy, free energy, and entropy, which are obtained from frequency calculations at the ωB97X-D/6-31G(d) level of theory, at 298 K and 1 atm.

Table 3. Thermochemical Parameters: Free Energy Adsorption (ΔG_{ads}), Enthalpy Adsorption (ΔH_{ads}) and Entropy Adsorption (ΔS_{ads}) Changes at T = 298.14 K and P = 1 atm with ωB97X-D/6-31G(d)

	ΔG_{ads} (kJ mol^{-1})	ΔH_{ads} (kJ mol^{-1})	ΔS_{ads} (J mol^{-1} K^{-1})
CNT(5.5)/Glyp	-11.59	-57.32	-153.09
BNNT(5.5)/Glyp	-14.89	-62.47	-159.33

All these thermochemical parameters are listed in Table 3. The negative value of ΔG_{ads} revealed that the glyphosate adsorption on CNT(5.5) and BNNT(5.5) was spontaneous and thermodynamically favourable. Moreover, the negative value of the thermal enthalpy adsorption (ΔH_{ads}) verifies the exothermic nature of glyphosate adsorption on the two nanotubes. While the negative values of the entropy (ΔS_{ads}) revealed a decrease in randomness due to glyphosate's immobilisation on the surface of the two nanotubes.

From the data in Table 3, we can conclude that all the thermodynamic parameters calculated for BNNT(5.5)/ glyphosate are more negative than those calculated for CNT(5.5)/glyphosate. In addition, glyp undergoes physical adsorption on the surfaces of nanotubes, indicating that the interaction existing between Glyp and the nanotubes is weak and of the van der Waals type.

To get more information about the nature of the intermolecular interaction of glyphosate and the two nanotubes, Bader's quantum theory of atoms in molecules (QTAIM) analysis was performed on the optimized geometries of two complexes using the ωB97X-D/6-31g(d) method by the Multiwfn program package.

It is worthy to note that the strength and the type of bonding between the attractive pairs of atoms are evaluated by knowing the value of ρ(r) (electron density) and the sign of $\nabla^2\rho(r)$ (Laplacian of electron density) at bond critical points (BCP).

All these BCP parameters for the two complexes are listed in Table 4, while Fig. 3 illustrates the calculated BCP with bond paths of two complexes.

In fact, from Table 4, we observe the existence of six BCPs for the two complexes. Positive Laplacian electron density values $\nabla^2\rho(r)$ with low electron density values confirm the non-covalent (van der Waals) interactions [41] between glyphosate and the two nanotubes.

In addition, to identify the nature of the intermolecular interaction, we observe the ratio G(r)/|V(r)| [42]. We find that all ratios of G(r)/|V(r)| > 1, this reveals that the interaction is non-covalent.

Accordingly, interactions between Glyp and nanotubes were identified as non-covalent. To get a deeper insight into these interactions, NCI analyses were performed by the Multiwfn package. The sign of (λ_2) could distinguish between bounded (sign (λ_2) < 0) and unbounded (sign (λ_2) > 0) [38].

In Fig. 4, we illustrate the density gradient versus the electron density multiplied by the sign of the second Hessian eigenvalue sign (λ_2). In this figure, we can observe that the adsorption of glyphosate on CNT(5.5) is characterised by the appearance of spikes over sign (λ_2) ≈ -0.01 a.u, whereas, for the adsorption of glyphosate on BNNT(5.5), the spikes appeared over sign (λ_2) ≈ -0.03 a.u (circled in red on Fig. 4). Thus, we noted that the interactions of both nanotubes are vdW in nature (sign (λ_2) < 0), however the high electron density of the spikes observed for the BNNT(5.5)/glyphosate complex shows that the glyphosate interaction with BNNT(5.5) is slightly stronger than that of CNT(5.5)/glyphosate, which is in agreement with a high level of adsorption energy determined in the case of BNNT(5.5)/glyphosate.

Table 4. The QTAIM Topological Parameters at the BCPs: λ_n (Eigenvalues of the Hessian Matrix of ρ, ρ(r) (Electron Density), $\nabla^2\rho(r)$ (Laplacian of Electron Density), G(r) (the Kinetic Electron Density) and V(r) (Potential Electron Density), Calculated with at the ωB97X-D/6-31G(d) Level. Values are in Atomic Units

System	Bond	λ_1	λ_2	λ_3	ρ(r)	$\nabla^2\rho(r)$	G(r)	V(r)	$\frac{G(r)}{\lvert V(r)\rvert}$
CNT (5.5) /Glyphosate	H_{91}-C_2	0.0699	-0.0132	-0.0118	0.0135	0.0448	0.0101	-0.0089	1.135
	O_{94}-H_{80}	0.0605	-0.0109	-0.0101	0.0114	0.0394	0.0091	-0.0083	1.096
	O_{94}-H_{79}	0.0569	-0.0097	-0.0100	0.0103	0.0372	0.0084	-0.0075	1.120
	N_{84}-H_{79}	0.0191	-0.0017	-0.0030	0.0047	0.0144	0.0029	-0.0024	1.208
	O_{96}-C_{23}	0.0183	-0.0025	-0.0008	0.0042	0.0149	0.0030	-0.0024	1.250
	H_{98}-C_{24}	0.0562	-0.0046	-0.0103	0.0112	0.0413	0.0087	-0.0072	1.208
BNNT(5.5)/ Glyphosate	H_{91}-N_{50}	0.1787	-0.0044	-0.0451	0.0329	0.0891	0.0238	-0.0254	0.937
	O_{94}-N_{28}	0.0321	-0.0022	-0.0048	0.0073	0.0251	0.0055	-0.0047	1.170
	N_{84}-N_{30}	0.0198	-0.0022	-0.0031	0.0048	0.0145	0.0032	-0.0028	1.143
	N_{84}-N10	0.0206	-0.0021	-0.0031	0.0050	0.0153	0.0034	-0.0030	1.133
	O_{97}-H_{78}	0.0339	-0.0057	-0.0016	0.0079	0.0265	0.0059	-0.0051	1.157
	O_{96}-N_{10}	0.0361	-0.0012	-0.0059	0.0081	0.0289	0.0060	-0.0048	1.250

CONCLUSIONS

We fulfilled the first-principle investigation of the adsorption of glyphosate on CNT(5.5) and BNNT(5.5) armchairs using the B3LYP, M06-2X and ωB97X-D/6-31G(d). Based on the results of the thermodynamics parameters, the interaction between glyphosate and both nanotubes undergoes a physisorption process that is exothermic and spontaneous. The negative value of the entropy change indicated an ordered arrangement of glyphosate on nanotubes. The QTAIM analysis exhibited that the intermolecular interactions between glyphosate and the two nanotubes are non-covalent. Besides, NCI analyses revealed that the related bonded interactions are of the van der Waals type.

The adsorption energy of BNNT(5.5)/glyphosate was slightly higher than that of CNT(5.5)/glyphosate that was in good agreement with the NCI analyses, where spikes appeared at high electron density in the case of BNNT(5.5)/glyphosate compared to CNT(5.5)/glyphosate. Moreover, the density of states of BNNT(5.5), after adsorption of glyphosate, showed a slight increase in the intensity of the peaks than that observed in the case of CNT, which is confirmed by the decrease in E_g after glyphosate adsorption on BNNT(5.5), whereas in the case of CNT(5.5)/glyphosate, the E_g was not affected after adsorption. This change in conduction involved an electrical signal, indicating that glyphosate could be more sensed with BNNT(5.5) than CNT(5.5) through a physisorption process, which is very convenient to detect hazardous substances due

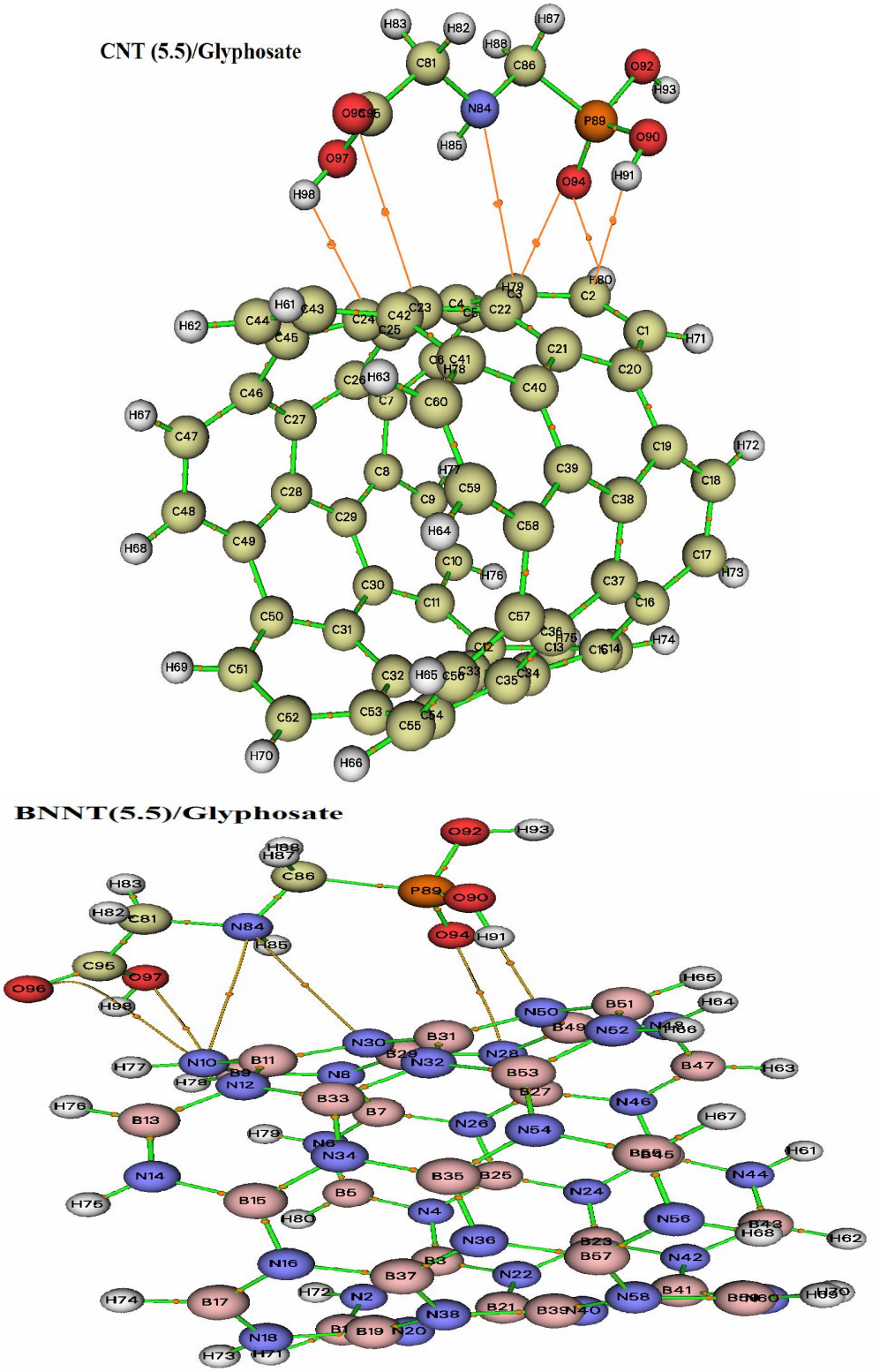

Fig. 3. The bond critical points (BCPs, orange spots), and bond paths (brown lines) for glyphosate adsorption onto the nanotubes.

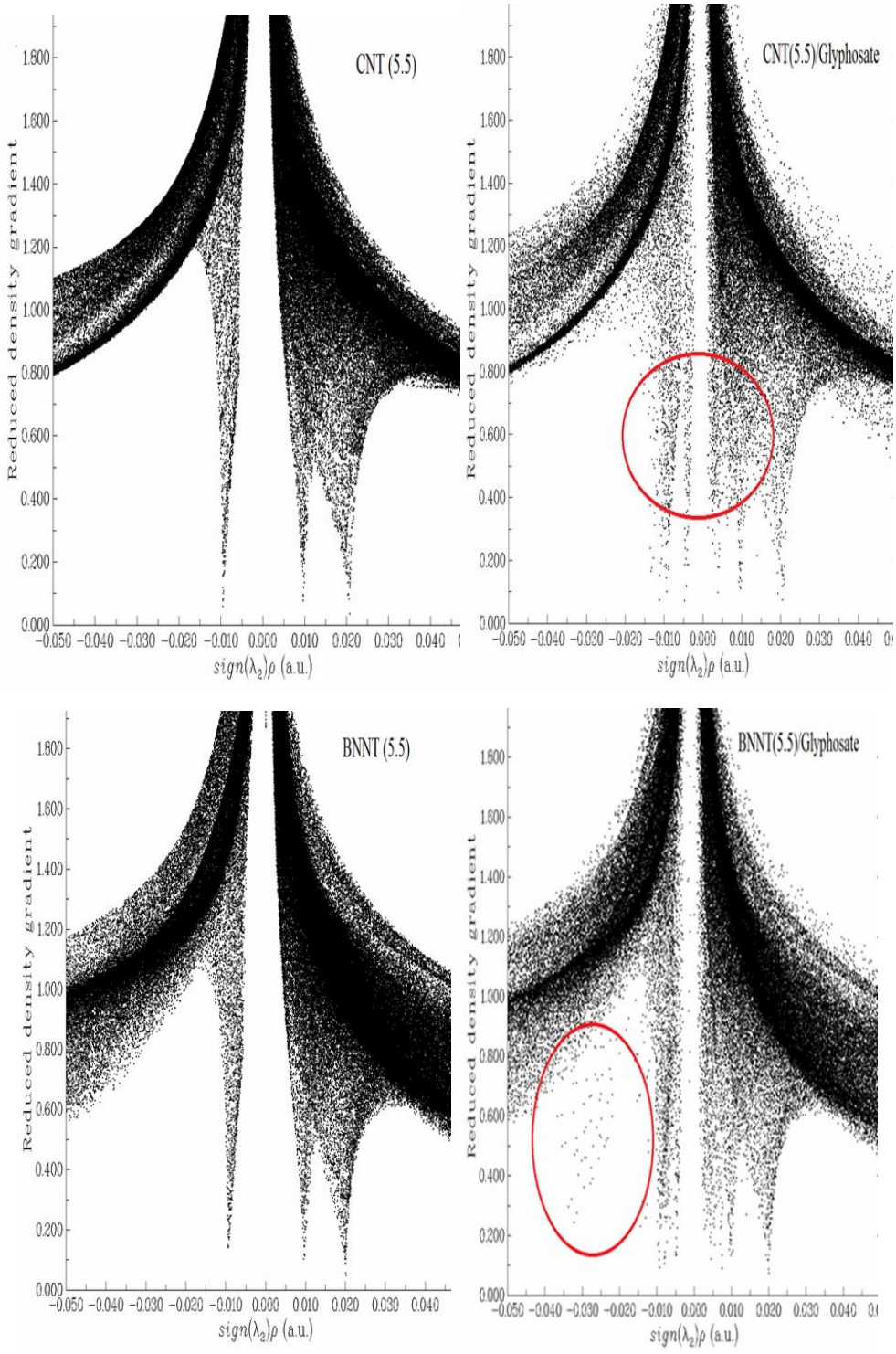

Fig. 4. Reduced density gradient (RDG) in function of sign $(\lambda_2)\rho$ for nanotubes and nanotube/glyphosate complexes calculated at the ωB97X-D/6-31G(d) level.

to the easy operation of desorption and it also allows the reuse of the nanotubes.

ACKNOWLEDGEMENTS

We gratefully acknowledge the financial support from The National School of Built and Ground Works Engineering, Kouba, Algiers, Algeria.

REFERENCES

[1] Cikalo, M. G.; Goodall, D. M.; Matthews W., Analysis of glyphosate using capillary electrophoresis with indirect detection. *J. Chroma. A*. **1996**, *745*, 189-200. DOI: 10.1016/0021-9673(96)00265-8.

[2] Mercurio, P.; Flores, F.; Mueller, J. F.; Carter, S.; Negri, A. P., Glyphosate persistence in seawater. *Mar. Poll. Bull.* **2014**, *85*, 385-90. DOI: 10.1016/j.marpolbul.2014.01.021.

[3] Battaglin, W. A.; Meyer, M. T.; Kuivila, K. M.; Dietze, J. E., Glyphosate and its degradation product AMPA occur frequently and widely in U.S. soils, surface water, groundwater, and precipitation. *J. Am. Water Resour. Assoc.* **2014**, *50*, 275-90. DOI: 10.1111/jawr.12159.

[4] Bai, S. H.; Ogbourne, S. M., Glyphosate: environmental contamination, toxicity and potential risks to human health *via* food contamination. *Environ. Sci. Poliut. Res.* **2016**, *23*, 18988-19001. DOI: 10.1007/s11356-016-7425-3.

[5] Bento, C. P. M.; Yang, X.; Gort, G.; Xue, S.; van Dam, R.; Zomer, P.; et al. Persistence of glyphosate and aminomethylphosphonic acid in loess soil under different combinations of temperature, soil moisture and light/darkness. *Sci. Tot. Environ*. **2016**, *572*, 301-11. DOI: 10.1016/j.scitotenv.2016.07.215.

[6] Guyton, K. Z.; Loomis, D.; Grosse, Y.; El Ghissassi, F.; Benbrahim-Tallaa, L.; Guha, N.; *et al.* Carcinogenicity of tetrachlorvinphos, parathion, malathion, diazinon, and glyphosate. *The Lancet Oncol.* **2015**, *16*, 490-1. DOI: 10.1016/S1470-2045(15)70134-8.

[7] Mesnage, R.; Defarge, N.; Spiroux de Vendômois, J.; Séralini, G. E., Potential toxic effects of glyphosate and its commercial formulations below regulatory limits. *Food and Chem. Tox.* **2015**, *84*, 133-53. DOI: 10.1016/j.fct.2015.08.012.

[8] Pu, Y.; Yang, J.; Chang, L.; Qu, Y.; Wang, S.; Zhang, K.; *et al.* Maternal glyphosate exposure causes autism-like behaviors in offspring through increased expression of soluble epoxide hydrolase. *Proc. Natl. Acad. Sci. USA*. **2020**, *117*, 11753-9. DOI: 10.1073/pnas.1922287117.

[9] Patnaik, P., Handbook of Environmental Analysis: Chemical Pollutants in Air, Water, Soil, and Solid Wastes, Second Edition. CRC Press, 2010.

[10] Gui, M.; Jiang, J.; Wang, X.; Yan, Y.; Li, S.; Xiao, X.; *et al.* Copper ion-mediated glyphosate detection with N-heterocycle based polyacetylene as a sensing platform. *Sensor. Actuat. B: Chem.* **2017**, *243*, 696-703. DOI: 10.1016/j.snb.2016.12.037.

[11] Jan, M. R.; Shah, J.; Muhammad, M.; Ara, B., Glyphosate herbicide residue determination in samples of environmental importance using spectrophotometric method. *J. Hazard. Mat.* **2009**, *169*, 742-5. DOI: 10.1016/j.jhazmat.2009.04.003.

[12] Xue, W.; Zhang, G.; Xu, X.; Yang, X.; Liu, C.; Xu, Y., Preparation of titania nanotubes doped with cerium and their photocatalytic activity for glyphosate. *Chem. Eng. J.* **2011**, *167*, 397-402. DOI: 10.1016/j.cej.2011.01.007.

[13] Çetin, E.; Şahan, S.; Ülgen, A.; Şahin, U., DLLME-spectrophotometric determination of glyphosate residue in legumes. *Food Chem.* **2017**, *230*, 567-71. DOI: 10.1016/j.foodchem.2017.03.063.

[14] Garcia, A. F.; Rollemberg, M. do. C., Voltammetric determination of glyphosate in natural waters with a copper electrode. *Quím. Nova.* **2007**, *30*, 1592-6. DOI: 10.1590/S0100-40422007000700018.

[15] Zouaoui, F.; Bourouina-Bacha, S.; Bourouina, M.; Abroa-Nemeir, I.; Ben Halima, H.; Gallardo-Gonzalez, J.; *et al.*, Electrochemical impedance spectroscopy determination of glyphosate using a molecularly imprinted chitosan. *Sensor. Actuat. B: Chem.* **2020**, *309*, 127753-74. DOI: 10.1016/j.snb.2020.127753.

[16] Zhou, X.; Tian, W. Q.; Wang, X. -L., Adsorption sensitivity of Pd-doped SWCNTs to small gas

molecules. *Sensor. Actuat. B: Chem.* **2010**, *151*, 56-64. https://doi.org/10.1016/j.snb.2010.09.054.

[17] Beheshtian, J.; Kamfiroozi, M.; Bagheri, Z.; Peyghan, A. A., $B_{12}N_{12}$ Nano-cage as potential sensor for NO_2 detection. *Chinese J. Chem. Phys.* **2012**, *25*, 60-4. https://doi.org/10.1088/1674-0068/25/01/60-64.

[18] Zeng, W.; Liu, T.; Wang, Z., Impact of Nb doping on gas-sensing performance of TiO_2 thick-film sensors. *Sensor. Actuat. B: Chem.* **2012**, *166-167*, 141-9. https://doi.org/10.1016/j.snb.2012.02.016.

[19] Beheshtian, J.; Bagheri, Z.; Kamfiroozi, M.; Ahmadi, A., Toxic CO detection by $B_{12}N_{12}$ nanocluster. *Microelectronics J.* **2011**, *42*, 1400-3. https://doi.org/10.1016/j.mejo.2011.10.010.

[20] Moraes, F. C.; Mascaro, L. H.; Machado, S. A. S.; Brett, C. M. A., Direct electrochemical determination of glyphosate at copper phthalocyanine/multiwalled carbon nanotube film electrodes. *Electroanalysis.* **2010**, n/a-n/a. DOI: 10.1002/elan.200900614.

[21] Oliveira, G. C.; Moccelini, S. K.; Castilho, M.; Terezo, A. J.; Possavatz, J.; Magalhães, M. R. L.; *et al*., Biosensor based on atemoya peroxidase immobilised on modified nanoclay for glyphosate biomonitoring. *Talanta.* **2012**, *98*, 130-6. DOI: 10.1016/j.talanta.2012.06.059.

[22] Chang, Y. C.; Lin, Y. S.; Xiao, G. T.; Chiu, T. C.; Hu, C. C., A highly selective and sensitive nanosensor for the detection of glyphosate. *Talanta.* **2016**, *161*, 94-8. DOI: 10.1016/j.talanta.2016.08.029.

[23] Tan, N.; Yang, Z.; Gong, X.; Wang, Z.; Fu, T.; Liu, Y., *In situ* generation of H_2O_2 using MWCNT-Al/O_2 system and possible application for glyphosate degradation. *Sci. Tot. Environ.* **2019**, *650*, 2567-76. DOI: 10.1016/j.scitotenv.2018.09.353.

[24] Zhang, Y.; Dang, Y.; Lin, X.; An, K.; Li, J.; Zhang, M., Determination of glyphosate and glufosinate in corn using multi-walled carbon nanotubes followed by ultra high performance liquid chromatography coupled with tandem mass spectrometry. *J. Chromat. A.* **2020**, *1619*, 460939. DOI: 10.1016/j.chroma.2020.460939.

[25] Blasé, X.; Rubio, A.; Louie, S. G.; Cohen, M. L., Stability and band gap constancy of boron nitride nanotubes. *EPL.* **1994**, *28*, 335-340. DOI: 10.1209/0295-5075/28/5/007.

[26] Chopra, N. G.; Luyken, R. J.; Cherrey, K.; Crespi, V. H.; Cohen, M. L.; Louie, S. G.; *et al.* Boron nitride nanotubes. *Science.* **1995**, *269*, 966-7. DOI: 10.1126/science.269.5226.966.

[27] Ganji, M. D.; Rezvani, M., Boron nitride nanotube based nanosensor for acetone adsorption: A DFT simulation. *J. Mol. Model.* **2013**, *19*, 1259-65. DOI: 10.1007/s00894-012-1668-9.

[28] Beheshtian, J.; Peyghan, A. A.; Bagheri, Z., Detection of phosgene by Sc-doped BN nanotubes: A DFT study. *Sensor. Actuat. B: Chem.* **2012**, *171-172*, 846-52. DOI: 10.1016/j.snb.2012.05.082.

[29] Yoosefian, M.; Etminan, N.; Moghani, M. Z.; Mirzaei, S.; Abbasi, S., The role of boron nitride nanotube as a new chemical sensor and potential reservoir for hydrogen halides environmental pollutants. *Superlatt. Microstr.* **2016**, *98*, 325-31. DOI: 10.1016/j.spmi.2016.08.049.

[30] Zhi, C.; Bando, Y.; Tang, C.; Golberg, D., Boron nitride nanotubes. *Mat. Sci. Eng.: R: Reports.* **2010**, *70*, 92-111. https://doi.org/10.1016/j.mser.2010.06.004.

[31] TubeGen Online-v3.4 n.d. https://turin.nss.udel.edu/research/tubegenonline.html (accessed May 27, 2020).

[32] Gaussian 16, Revision A.03, M. J.; Frisch, G. W.; Trucks, H. B.; Schlegel, G. E.; Scuseria, M. A.; Robb, J. R.; Cheeseman, G.; Scalmani, V.; Barone, G. A.; Petersson, H.; Nakatsuji, X.; Li, M.; Caricato, A. V.; Marenich, J.; Bloino, B. G.; Janesko, R.; Gomperts, B.; Mennucci, H. P.; Hratchian, J. V.; Ortiz, A. F.; Izmaylov, J. L.; Sonnenberg, D.; Williams-Young, F. Ding, F.; Lipparini, F.; Egidi, J.; Goings, B.; Peng, A.; Petrone, T.; Henderson, D.; Ranasinghe, V. G.; Zakrzewski, J.; Gao, N.; Rega, G.; Zheng, W.; Liang, M.; Hada, M.; Ehara, K.; Toyota, R.; Fukuda, J.; Hasegawa, M.; Ishida, T.; Nakajima, Y.; Honda, O.; Kitao, H.; Nakai, T.; Vreven, K.; Throssell, J. A.; Montgomery, Jr., J. E.; Peralta, F.; Ogliaro, M. J.; Bearpark, J. J.; Heyd, E. N.; Brothers, K. N.; Kudin, V. N.; Staroverov, T. A.; Keith, R.; Kobayashi, J.; Normand, K.; Raghavachari, A. P.; Rendell, J. C.; Burant, S. S.; Iyengar, J.; Tomasi, M.; Cossi, J. M.; Millam, M.; Klene, C.;

Adamo, R.; Cammi, J. W.; Ochterski, R. L.; Martin, K.; Morokuma, O.; Farkas, J. B.; Foresman, D. J., Fox, Gaussian, Inc., Wallingford CT, 2016, n.d.

[33] Dai, B. Q.; Zhang, G. L.; Zhao, J. X., A DFT/B3LYP Computational study of boron-nitride nanotubes. *Jnl. Chinese. Chem. Soc.* **2003**, *50*, 525-8. DOI: 10.1002/jccs.200300077.

[34] Kar, T.; Akdim, B.; Duan, X.; Pachter, R., A theoretical study of functionalised single-wall carbon nanotubes: ONIOM calculations. *Chem. Phys. Lett.* **2004**, *392*, 176-80. DOI: 10.1016/j.cplett.2004.05.015.

[35] Wang, Y.; Verma, P.; Zhang, L.; Li, Y.; Liu, Z.; Truhlar, D. G.; *et al*., M06-SX screened-exchange density functional for chemistry and solid-state physics. *Proc. Natl. Acad. Sci. USA.* **2020**, *117*, 2294-301. DOI: 10.1073/pnas.1913699117.

[36] Chai, J. D.; Head-Gordon, M., Long-range corrected hybrid density functionals with damped atom-atom dispersion corrections. *Phys. Chem. Chem. Phys.* **2008**, *10*, 6615-20. DOI: 10.1039/b810189b.

[37] Bader, R. F. W., A quantum theory of molecular structure and its applications. *Chem. Rev.* **1991**, *91*, 893-928. DOI: 10.1021/cr00005a013.

[38] Johnson, E. R.; Keinan, S.; Mori-Sánchez, P.; Contreras-García, J.; Cohen, A. J.; Yang, W., Revealing noncovalent interactions. *J. Am. Chem. Soc.* **2010**, *132*, 6498-506. DOI: 10.1021/ja100936w.

[39] Tian, L.; Feiwu, C., Multiwfn: A multifunctiona wavefunction analyzer, *J. Comput. Chem.* **2012**, *33*, 580-592. DOI: 10.1002/jcc.22885.

[40] Salvador, P.; Paizs, B.; Duran, M.; Suhai, S., On the effect of the BSSE on intermolecular potential energy surfaces. Comparison ofa priori anda posteriori BSSE correction schemes. *J. Comput. Chem.* **2001**, *22*, 765-86. https://doi.org/10.1002/jcc.1042.

[41] Bohórquez, H. J.; Boyd, R. J.; Matta, C. F., Molecular model with quantum mechanical bonding information. *J. Phys. Chem. A.* **2011**, *115*, 12991-7. DOI: 10.1021/jp204100z.

[42] Nemati-Kande, E.; Karimian, R.; Goodarzi, V.; Ghazizadeh, E., Feasibility of pristine, Al-doped and Ga-doped Boron Nitride nanotubes for detecting SF_4 gas: A DFT, NBO and QTAIM investigation. *Appl. Surf. Sci.* **2020**, *510*, 145490-512. DOI: 10.1016/j.apsusc.2020.145490.